

Surface-stress effects on elastic properties. II. Metallic multilayers

F. H. Streitz*

Department of Physics and Astronomy, The Johns Hopkins University, Baltimore, Maryland 21218

R. C. Cammarata and K. Sieradzki

Department of Materials Science and Engineering, The Johns Hopkins University, Baltimore, Maryland 21218

(Received 8 April 1993)

In the adjoining paper we presented a detailed model describing the effects of surface stress on the equilibrium spacing and biaxial modulus of thin metal films. We extend the model to describe the effects of interface stress on metallic multilayers. The model predicts that very thin layers will equilibrate to a spacing in the plane smaller than the bulk spacing for the material, and that this effect will vanish as the reciprocal of the layer thickness. The model predicts enhancements in the biaxial modulus of metallic multilayers which scale with the reciprocal of the layer thickness. The magnitude of both the strain and the resulting change in biaxial modulus are proportional to the magnitude of the interface stress. In order to verify the predictions of the interface stress model, we performed molecular-dynamics computer simulations of metallic multilayers using the "universal" form of the embedded-atom-method (EAM) potentials, an analytic form of the EAM potential, and a slightly modified version of the analytic form. The model was found to predict accurately the equilibrium properties of metallic multilayers. We discuss the limitations of the EAM potentials and the implications of this work for the supermodulus effect.

I. INTRODUCTION

The elastic properties of artificially multilayered metallic thin films have been the subject of a great deal of interest since the first reports,¹⁻³ of significant enhancements in certain elastic moduli of these materials when the bilayer repeat length λ was reduced to about 2 nm. These reports of the so-called supermodulus effect involved increases of 100% or more in the in-plane biaxial moduli of Au-Ni¹, Cu-Ni², and Ag-Pd.⁴ In the case of Cu-Ni and Ag-Pd, an in-plane biaxial modulus approaching that of diamond was reported. Since its initial announcement, the supermodulus effect has been highly controversial. The investigations cited above involved measurements of the biaxial modulus by a bulge tester, and a detailed study of the actual apparatus used suggested that the supermodulus effect was in fact an experimental artifact.⁴ More accurate methods for measuring elastic properties of thin films have recently been perfected involving ultrasonic and nanoindentation techniques. Investigations using these methods have revealed that much smaller variations in elastic moduli (both enhancements and reductions of about 5–50%) do exist in certain multilayered films, such as Ag-Pd (Ref. 5) and Cu-Nb;⁶ however, two of the original supermodulus systems, Cu-Pd (Refs. 7–9) and Cu-Ni (Refs. 10 and 11) showed no variations in elastic behavior with λ .

Recently, several atomistic computer simulations have been performed to investigate the elastic properties of metallic superlattices possessing both coherent (lattice matched) and noncoherent (non-lattice-matched) interfaces.¹²⁻¹⁷ None of these investigations produced elastic anomalies similar in magnitude to the original supermodulus reports, but some of the simulations resulted in the smaller modulus variations characteristic of the behavior

reported in the more recent experimental studies. While there has been some disagreement as to whether there is any effect in coherent superlattices, most of the simulations involving noncoherent superlattices have displayed modulus variations when λ is reduced to about 2 nm.

It has been suggested that the origin of elastic modulus variations in multilayered metallic materials is based on interface stress effects.¹⁸ Interface stresses induce large elastic strains when the individual layer thickness is of order 1 nm, resulting in higher-order elastic effects that are manifested in the effective elastic moduli. Since it is expected that noncoherent interfaces will have interface stresses larger in magnitude than coherent interfaces,¹⁸ more significant modulus anomalies are expected in noncoherent superlattices as compared to coherent ones. In this paper, effects of interface stresses on the structural and elastic behavior of both coherent and noncoherent superlattices are investigated.

II. INTERFACE STRESS MODEL

The arguments leading to the surface-stress model (discussed in Ref. 19, henceforth referred to as I) are equally valid when applied to a thin layer which is subject to interface stress. The equations derived are identical as long as one redefines certain parameters in order to properly account for the new geometry. Consider a metallic multilayer, shown schematically in Fig. 1. The composition modulation wavelength in a multilayer is defined as the distance over which the composition repeats, and will be denoted by λ_0 . This quantity is the analog to the film thickness of a thin film. The reference biaxial modulus of the multilayer assembly is defined in a manner similar to that used in I: Y_∞ is taken to be the biaxial modulus of the structure in the limit of an infinitely thick modulation wavelength. Note that for a thin film, this definition

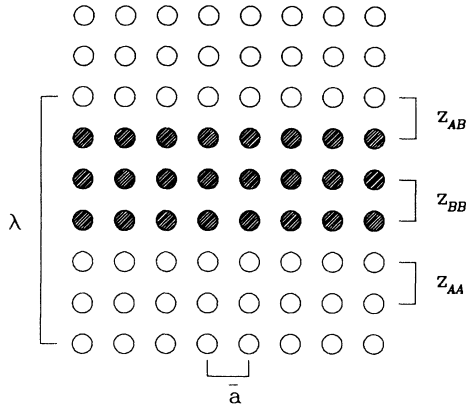


FIG. 1. Schematic of a metallic multilayer, defining the composition modulation wavelength λ_0 , the in-plane spacing \bar{a} , and the atomic separations z , z_{BB} , and z_{AB} .

leads to Y_∞ being equal to the bulk biaxial modulus, while for a multilayer Y_∞ is defined as the volume average of the bulk biaxial moduli of the constituents.^{20,21}

Using the definition of λ_0 given above, and recognizing that Y_∞ represents a volume average of bulk quantities, we can write the relevant equations for the interface stress model by rewriting Eqs. (17) and (20) from I:

$$\varepsilon^* \approx \frac{-2f_0}{4f_0 + 2f' + \lambda_0 Y_\infty} \sim \frac{-2f_0}{\lambda_0 Y_\infty} \quad (1)$$

and

$$Y(\lambda_0) = Y_\infty + \frac{2f_0}{\lambda_0} (B_\infty + 2\eta - 3 + f'/f_0), \quad (2)$$

where f_0 is the interface stress and f' the strain derivative of the interface stress. The quantities B_∞ and η describe how the biaxial modulus and the thickness, respectively, vary with strain. The biaxial modulus can be expanded in the normal way to include higher-order elastic constants such as B_∞ and C_∞ :

$$Y(\varepsilon, \lambda = \infty) = Y_\infty (1 - B_\infty \varepsilon + \frac{1}{2} C_\infty \varepsilon^2 + \dots), \quad (3)$$

while the thickness of a layer will respond in a Poisson-like fashion to a biaxial strain:

$$\lambda(\varepsilon) = \lambda_0 (1 - \eta \varepsilon), \quad (4)$$

which reflects the two predictions made by the model: that the in-plane spacing and biaxial modulus of a layered structure will vary with layer thickness, and the exact nature of that variation will depend on the interface stress. Equations (1) and (2) predict that very thin layers in a metallic multilayer will equilibrate to an in-plane spacing smaller than their bulk spacing due to the presence of an interface stress, and that this equilibrium biaxial strain will result in changes in the elastic properties of the multilayer assembly.

III. COMPUTER SIMULATION OF METALLIC MULTILAYERS

We performed molecular-dynamics simulations of transition-metal multilayers following the same steps outlined in I for the simulation of thin films. After creating a sample in an initial configuration, we equilibrated the sample by slowly removing kinetic energy while allowing the system to evolve using a Parrinello-Rahman Lagrangian.²² After the sample had reached equilibrium (at a temperature which was nominally zero), we applied a series of small biaxial stresses to the sample and measured the resulting strains. The total energy of the sample was recorded during the simulation, so that at the finish of a sample run we had a stress-strain curve and a strain-energy curve for the multilayer. From this point analysis could proceed as outlined in I.

The initial configuration of a multilayer (either coherent or noncoherent) involved the input of four spacings: the in-plane spacing \bar{a} , the interplanar separations between similar materials z_{AA} and z_{BB} , and the interplanar separation between dissimilar materials, z_{AB} . These spacings are depicted in Fig. 1.

The initial in-plane spacing for a coherent sample was taken to be the average of the bulk spacing of the two constituents. The initial value of \bar{a} for a noncoherent multilayer was taken to be the bulk spacing of either material, with the in-plane spacing for the other material forced by the boundary conditions to be a rational fraction of the first. Periodic boundary conditions constrain the atoms at a noncoherent interface to maintain their original registry. Thus if m -type A atoms are aligned with n -type B atoms, we could pick the initial value of \bar{a}_A to be the A bulk spacing (with \bar{a}_B equal to m/n of the A spacing), or we could assign \bar{a}_B to be the bulk B atom spacing, in which case the A atoms would start at an in-plane spacing of n/m times the B spacing. The residual misfit ε_m is given by

$$\varepsilon_m = 2 \left(\frac{ma_A - na_B}{ma_A + na_B} \right). \quad (5)$$

For appropriate choices of n and m , typical values of ε_m are small (around 0.5%), and the multilayers would approach the same equilibrium state with either choice of initial spacing.

The values of m and n are chosen by taking the ratio of integers closest to the ratio a_A/a_B . For example, in the case of silver and nickel, a_{Ag}/a_{Ni} is 1.1619. The smallest set of integers with this ratio is 7 and 6, $7/6 = 1.1666$. (Note that $6a_{Ag} < 7a_{Ni}$, so that the residual misfit strain will tend to expand the silver and compress the nickel, despite the fact that silver has the larger atomic spacing.)

The residual misfit strain is an artifact of the computation sample size. The misfit strain described above using $m=6$ and $n=7$ for silver and nickel results in $\varepsilon_m = -0.004$. A better choice of integers would have been $m=37$ and $n=43$, which results in a residual misfit strain of $\varepsilon_m = 0.0002$. Such a sample would have required over 40 times as much computer time to investigate, which necessitated the use of the smaller sample.

IV. INTERATOMIC POTENTIALS

We utilized three related embedded-atom-method (EAM) potentials in our study of metallic multilayers: the “universal” EAM potentials of Daw and Baskes²³ and Foiles, Daw, and Baskes,²⁴ an analytic form of EAM potential developed for fcc metals by Johnson,^{25,26} and a form of this latter potential which the authors modified in order to more closely describe the magnitude of the surface stress.²⁷ As the first two forms have been extensively described in the literature, we will not further describe them here. Wüttig, Franchy, and Ibach²⁸ estimated the surface stress on a (001) surface of Ni from discrepancies in phonon-dispersion curves, calculating a value of $0.16 \text{ eV}/\text{\AA}^2$. Menezes *et al.*³⁶ used a similar argument to calculate the surface stress on the (111) Ni surface, which they found to be $0.10 \pm 0.01 \text{ eV}/\text{\AA}^2$. These observations remain the only experimentally based values of surface stress for a particular crystallographic plane in metals to date. Table I compares the surface energies and surface stresses calculated for the (001) and (111) surfaces of nickel using both the “universal” EAM and analytic EAM potential, along with experimental or theoretical results where available. While both potentials yield essentially the same (incorrect) value of surface energy, we see that their predictions for surface stress disagree substantially, both among themselves and with the experimental values. The analytic potential is seen to be incorrect by almost exactly a factor of 2 in γ and f for both surfaces, while the universal EAM potential depends sensitively on the surface. Thus, while comparisons between different metals modeled using the same potential are possible, one should take care when comparing any results attained using different forms of embedded-atom potential. It is well known that these EAM potentials cannot accurately reproduce surface energies, although it is often argued that they reproduce trends across the transition elements correctly.^{24,25,30} It is less well appreciated that the surface-stress values are very potential specific. Gumbsch and Daw calculated surface energies and stresses for several fcc transition elements using universal EAM potentials, and compared their work to some of the *ab initio* calculations available, as well as to results obtained with other EAM-like potentials, such as the Finnis-Sinclair potential.^{31,32} They noted the same discrepancies which we mentioned above, concluding

TABLE I. Surface energies and stresses for nickel (001) and (111) surfaces calculated with universal and analytic version of the EAM potential, compared with previous experimental or theoretical work where possible. All units are $\text{eV}/\text{\AA}^2 = 16.022 \text{ J}/\text{m}^2$.

	Universal	Analytic	Previous work
γ_{111}	0.090	0.083	0.15 ^a
f_{111}	0.027	0.051	0.10 ^b
γ_{001}	0.098	0.097	0.19 ^a
f_{001}	0.079	0.047	0.12 ^c

^aReference 33.

^bReference 28.

^cReference 29.

TABLE II. Nickel input parameters for analytic and modified potentials, including the resulting values of the bulk modulus (K), shear modulus (G), vacancy formation energy (E_v), surface energy (γ_{111}), and surface stress (f_{111}). ($\text{eV}/\text{\AA}^3 = 1.6022 \times 10^{11} \text{ J}/\text{m}^3$, $\text{eV}/\text{\AA}^2 = 16.022 \text{ J}/\text{m}^2$).

	Ni(111)	“Ni”(111)
α	4.98	5.80
β	6.41	5.10
γ	8.86	8.10
$a(\text{\AA})$	3.5196	3.5196
E_c (eV)	4.45	4.45
E_v (eV)	1.70	2.62
K ($\text{eV}/\text{\AA}^3$)	1.13	1.53
G ($\text{eV}/\text{\AA}^3$)	0.59	0.66
γ_{111} ($\text{eV}/\text{\AA}^2$)	0.083	0.133
f_{111} ($\text{eV}/\text{\AA}^2$)	0.051	0.104

that they “should emphasize qualitative conclusions rather than precise numerical results.”³⁰

We felt that it would be instructive to alter the analytic EAM potentials so that the materials modeled would exhibit more realistic values of surface energy and surface stress. By altering the exponents α , β , and γ which are input parameters in the analytic EAM potentials, we can manipulate the curvature of the potentials and hence their surface stress. We created “Ni” and “Ag” potentials in this way. Tables II and III display the input parameters for the original analytic potential and the modified analytic potential, along with the resulting values of surface energy and stress, for (111) Ni and (111) Ag. The final values for α , β , and γ were obtained by trial and error, as an analytic expression for the surface energy was not obtainable. The “theoretical” value for the (111) surface stress of Ag was approximated by noting that in all cases the surface energy and stress calculated by using the analytic potential differed from either *ab initio* or experimental results by almost exactly a factor of 2. As there are neither *ab initio* nor experimental results for the (111) Ag surface, we simply attempted to double the original value. The modified materials are seen to have properties similar to the actual materials. The properties

TABLE III. Silver input parameters for analytic and modified potentials, including the resulting values of the bulk modulus (K), shear modulus (G), vacancy formation energy (E_v), surface energy (γ_{111}), and surface stress (f_{111}). ($\text{eV}/\text{\AA}^3 = 1.6022 \times 10^{11} \text{ J}/\text{m}^3$, $\text{eV}/\text{\AA}^2 = 16.022 \text{ J}/\text{m}^2$).

	Ag(111)	“Ag”(111)
α	5.92	7.60
β	5.96	4.75
γ	8.26	7.70
$a(\text{\AA})$	4.0896	4.0896
E_c (eV)	2.85	2.85
E_v (eV)	1.10	1.70
K ($\text{eV}/\text{\AA}^3$)	0.65	1.07
G ($\text{eV}/\text{\AA}^3$)	0.21	0.25
γ_{111} ($\text{eV}/\text{\AA}^2$)	0.043	0.077
f_{111} ($\text{eV}/\text{\AA}^2$)	0.063	0.121

which were seen to change the most were the bulk modulus, shear modulus, and vacancy formation energy. This is not surprising, as they are the three properties which were used as primary input parameters in the original potentials.²⁵ The change in bulk modulus, while severe for both materials, is irrelevant for the purpose of testing the model. These potentials were not intended to be used in a simulation of real Ni and Ag. Our intent in creating these potentials was to test the prediction of the model with a system which has greater (and hence more realistic) values of surface stress than those which result from the original potential.

V. RESULTS

We performed computer simulations on coherent and noncoherent fcc metallic multilayers using the "original" form of the EAM potential due to Foiles, Daw, and Baskes,²⁴ the analytic EAM potentials of Johnson,^{25,26} and a modified form of the analytic EAM potentials which predict correct values of surface stress, as discussed above.²⁷ Samples were created by juxtaposing in correct stacking sequence slabs of two different fcc metals (Cu-Ni, Cu-Pd, Au-Ni, or Ag-Ni) where each slab contained the same number of layers. The sample interfaces were oriented either (001) or (111). The multilayer interfaces were constrained to maintain coherence or incoherence by using periodic boundary conditions in place of the interface. Periodic boundary conditions perpendicular to the interfaces were used to remove any free surface effects. The unit cell for the simulation included exactly one repeat length in the direction of composition modulation. We studied samples of unit cell size 2 and 3 as well in order to insure that there were no finite-size effects. The coherent samples contained 50 atoms per (001) or 100 atoms per (111) layer. The unit cell size of the noncoherent samples depended on the sample. In the Au-Ni multilayers, the Au layers contained 128 atoms per (001) layer or 256 per (111) layer, and the Ni layers contained 98 atoms per (001) layer or 196 per (111) layer. In the Ag-Ni multilayers, the Ag layers contained 98 atoms per (001) layer or 196 per (111) layer, and the Ni layers contained 72 atoms per (001) layer or 144 per (111) layer. The equilibrium strain in a multilayered sample is defined with respect to the in-plane spacing at infinite layer thickness. For the coherent multilayers the in-plane spacing is \bar{a} , the common in-plane spacing for the two materials. For the noncoherent samples, equilibrium strain was defined relative to the area of the box at infinite layer thickness. Note that this would not be the bulk spacing of either material, due to the residual misfit strain.

A. Coherent multilayers

The nature of the interface, coherent vs noncoherent, will have a profound effect on the magnitude of the interface stress. Consider the local environment of an atom at a coherent or noncoherent interface. At a coherent interface, all of the atoms have the same (bulk) coordination.

The redistribution of electronic charge which occurs at the interface will be due solely to the chemical differences between the constituent materials. In-plane bonds situated near the interface will not differ significantly from similar bonds in the bulk. As surface stress is an excess quantity (as is γ), the surface stress for coherent interfaces will be small. By contrast, the environment of an atom at a noncoherent interface will be substantially different from the bulk. There will be a significant redistribution of electrons in the plane of the interface, due to the presence of dislocations, as well as the smaller contribution due to the chemical differences. As a result, interface stresses at a noncoherent interface will in general be much larger in magnitude than at a coherent interface. We studied three different coherent systems: copper-nickel, copper-palladium, and gold-nickel, ranked in order of increasing misfit strain ϵ_m , using the analytic form of EAM potential. The parameters Y_∞ , B_∞ , η , f_0 , and f' calculated for the coherent multilayers are presented in Table IV. A discussion of these results and a comparison with the predictions of the thermodynamic model follow.

We first note, however, that the interface energies for Au-Ni are negative even though the heat of mixing for this system is positive. This apparent discrepancy may be due to the fact that the nature of the interaction is strongly affected by the presence, in both metals, of the relatively large elastic strains needed to make a coherent interface. As discussed in Sec. V B, the noncoherent Au-Ni interface has a positive interface energy, as expected. One could also argue that the alloy potentials used are not sufficiently precise to distinguish between a very small *positive* γ and a very small *negative* γ . In any event, the simulations result in values of γ (as well as f and f') that have the expected order of magnitude, and therefore should be able to qualitatively describe the magnitude of their effect on the elastic behavior. Figure 2 displays the equilibrium biaxial strain ϵ^* and biaxial modulus Y_∞ , as a function of the composition modulation wavelength λ_0 for coherent Cu-Ni superlattices oriented (001) and (111). The extremely small values of surface stress for these coherent multilayers, about a factor of 10 smaller than typical surface stresses for free surfaces, results in essentially no change in the in-plane spacing as a function of the bilayer repeat length λ . The maximum strain is seen to be less than 0.1% in this system. The biaxial modulus is unchanged over the modulation wavelength range we studied, as we would expect given the small biaxial strains which develop. The Cu-Ni system is one of the most studied metallic multilayer systems, both experimentally and theoretically. Some of the original results on the supermodulus effect were for the Cu-Ni system,² and much of the previous theoretical work was performed on it.^{12,14,34} Recent experimental results have discounted the existence of a supermodulus effect in the Cu-Ni system, in agreement with this work and the previous theoretical work cited.⁹ Figure 3 displays the biaxial modulus for the (111)-oriented multilayers as a function of λ_0 , along with experimental and theoretical estimates. Aside from the unusual early experimental results, we see that our results are in good

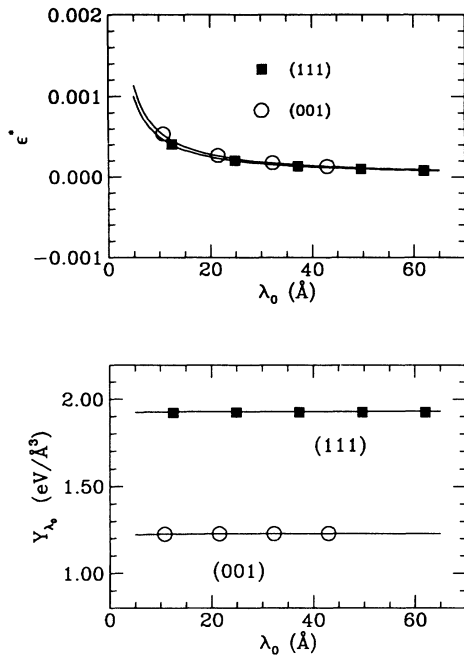


FIG. 2. Equilibrium biaxial strain ϵ^* and biaxial modulus Y_{λ_0} as functions of composition modulation wavelength λ_0 for coherent (001)- and (111)-oriented Cu-Ni multilayers.

agreement with the recent experimental work of Moreau, Ketterson, and Davis, and in almost perfect agreement with the computer simulations of Mintmire and co-workers, who studied coherent (111)-oriented Cu-Ni multilayers using the EAM potentials of Foiles, Daw, and Baskes.²⁴ Given the evidence, one is forced to conclude that there is no modulus enhancement in coherent multilayers of Cu-Ni as a function of composition wavelength.

Figure 4 depicts the equilibrium biaxial strain and bi-

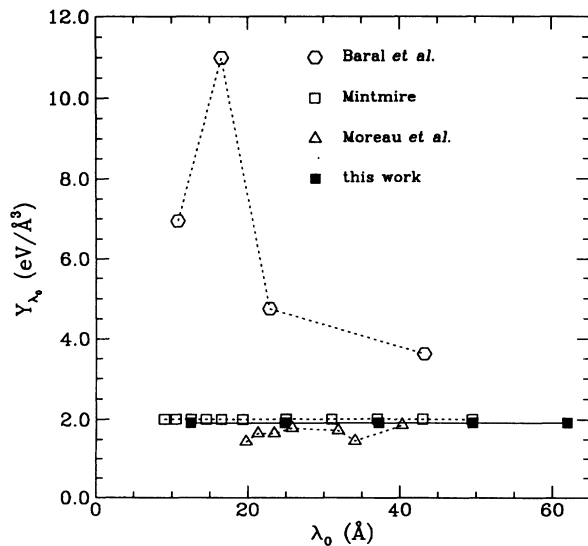


FIG. 3. Biaxial modulus Y_{λ_0} for coherent (111) Cu-Ni films, comparing our results with other experimental and theoretical work.

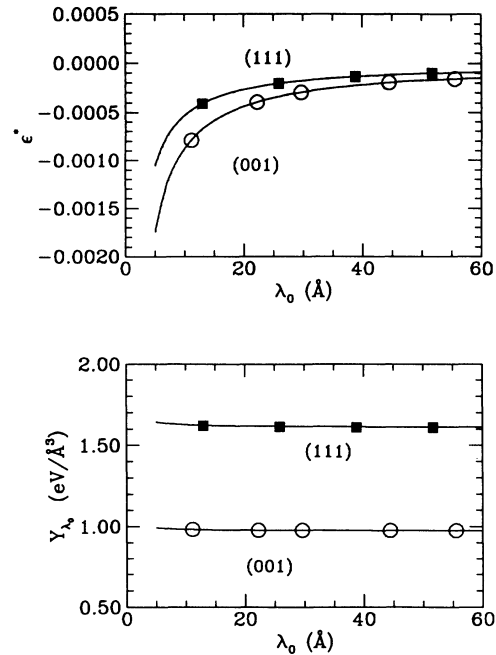


FIG. 4. Equilibrium biaxial strain ϵ^* and biaxial modulus Y_{λ_0} as functions of composition modulation wavelength λ_0 for coherent (001)- and (111)-oriented Cu-Pd multilayers.

axial modulus as a function of modulation wavelength for coherent Cu-Pd multilayers. The Cu-Pd system is unique among the systems we studied in that the stiffer material (Pd) has the larger spacing. ($a_{\text{Pd}} = 3.79$ Å and $a_{\text{Cu}} = 3.62$ Å). Thus, in this system, the stiffer material is forced to compress, while the softer material is required to expand in order to maintain coherence. Since the biaxial modulus increases with increasing compressive strain, coherency strain arguments would imply that by compressing the already stiffer material, the Cu-Pd multilayers should display large biaxial modulus enhancements as a function of composition wavelength. Unfortunately, that is not the case. The Pd compresses very little in the system, since the softer Cu can expand with a lower cost of energy. Since the surface stress is very low, which we would expect for a coherent system, there is again no modulus enhancement seen. Figure 4 shows that the values of equilibrium biaxial strain, while larger than those for the Cu-Ni system, are still well below 0.1%. It is no surprise, within the context of our thermodynamic model, that the biaxial modulus shows no variation with composition modulation wavelength. Figure 5 displays the biaxial modulus of (111) Cu-Pd as a function of from recent experimental⁷ and computer simulation results using the EAM potentials of Foiles, Daw, and Baskes²⁴ as well as our results. We see that although the scatter in the experimental data is large, the data are clearly centered on our results, and show no supermodulus effect. The computer simulation by Gilmore and Provenzano investigated much thinner samples than we did, and used a spherical sample geometry with free surfaces. Nevertheless, their results compare well with ours in predicting no supermodulus effect in the Cu-Pd system. They attribute

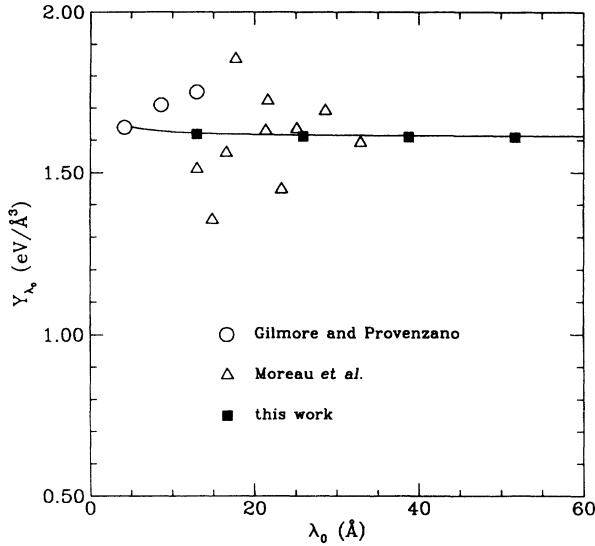


FIG. 5. Biaxial modulus Y_{λ_0} for coherent (111) Cu-Pd films, comparing our results with other experimental and theoretical work.

the small decrease in biaxial modulus which they observe with decreasing wavelength to the increasing coherence of these very thin samples. We attribute their slightly higher values of modulus to the presence of free surfaces.

The misfit in the Au-Ni system is 13.7%, which is twice as large as the misfit in the Cu-Pd system (7.1%) and more than five times as large as the misfit in the Cu-Ni system (2.6%). Table IV shows that the interface stress in the Au-Ni system has the largest value of any of the coherent systems we studied. The size of surface stress is not directly related to the size of the misfit strain, however. The origin of the surface stress in coherent structures, as discussed above, is the difference in the electronic makeup of the two materials, as the arguments based on loss of coordination do not apply at a coherent interface. Consider the Au-Ni system: within the framework of the embedded-atom method, the equilibrium electron density (ρ_0) is given by the cohesive energy (E_c) divided by the atomic volume (Ω). Nickel has a large cohesive energy ($E_c = -4.45$ eV), resulting in tight bonds ($\Omega = 10.9 \text{ \AA}^3$). Thus, in a nearest-neighbor model, where each bond contributes one-twelfth the total energy density, we see a value for $\rho_0 = 0.034 \text{ eV/\text{\AA}^3}$. For gold, the cohesive energy is almost as high ($E_c = -3.93$ eV) but

the volume is much larger, with $\Omega = 16.98 \text{ \AA}^3$. Thus each bond contributes $\rho_0 = 0.019 \text{ eV/\text{\AA}^3}$, almost a factor of 2 less density than the nickel. At a coherent interface, the juxtaposition of the two types of atoms leaves the nickel atoms at the surface starved for electron density, while the gold on the other side is suffering from an abundance of electron density. The simple response to this situation is for the gold atoms at the interface to try to expand (to reduce their local electron density), while the nickel atoms near the interface try to contract (in order to increase their local electron density). As usual, this surface-driven effect is counteracted by the volume energy that these changes would cost. Since nickel has the larger biaxial modulus (by a factor of 2), the system equilibrates at a spacing closer to the bulk spacing of nickel, leaving the gold atoms too close together. The bulk of the gold has to provide a compressive or negative surface stress in order to keep its surface atoms so close together. As the system becomes thinner, the volume strain energies are not as dominant, and the system relaxes to larger in-plane spacings. The equilibrium biaxial strain and biaxial modulus for the coherent Au-Ni multilayers as a function of modulation wavelength are shown in Fig. 6. The large values of interface stress manifest themselves in the large magnitude of the strains which develop in the plane. The strains are positive, as discussed above. The largest strains (for films with $\lambda_0 < 15 \text{ \AA}$) are approximately 0.5%. The biaxial modulus of the coherent Au-Ni system is virtually independent of composition modulation wavelength, despite the large stresses (and strains) which develop. As discussed in I, the presence of a surface stress is not sufficient to produce a variation in modulus. The second term in Eq. (2), which describes the variation in biaxial modulus with layer thickness, is the sum of three constants: B_∞ , η , and the ratio of f' to f_0 . This sum is multiplied by the surface stress to give the deviation from bulk in the biaxial modulus. The ratio of f'/f_0 is of the same order as $-B_\infty$ in this system, so that they sum to a small number. Thus the value of f' is seen to be important in determining the magnitude of the thickness dependence of the modulus.

There is no straightforward physical interpretation of the quantity f' . It is merely the first term in a Taylor expansion of surface stress about zero strain, as described in I. Since the deviation of a stress with respect to strain is a modulus, we can consider f' a "surface modulus." If

TABLE IV. Values of Y_∞ , B_∞ , η , γ , f_0 , f' , and ϵ_m determined from simulations of (001) and (111) multilayers of coherent Cu-Ni, Cu-Pd, and Au-Ni, as discussed in the text ($\text{eV/\text{\AA}^3} = 1.6022 \times 10^{11} \text{ J/m}^3$, $\text{eV/\text{\AA}^2} = 16.022 \text{ J/m}^2$).

	Y_∞ ($\text{eV/\text{\AA}^3}$)	B_∞	η	γ ($\text{eV/\text{\AA}^2}$)	f_0 ($\text{eV/\text{\AA}^2}$)	f' ($\text{eV/\text{\AA}^2}$)	ϵ_m (%)
Cu-Ni(001)	1.23	14.0	1.14	0.003	-0.004	0.03	2.7
Cu-Ni(111)	1.93	14.6	0.70	0.011	-0.005	0.05	2.7
Cu-Pd(001)	0.97	13.7	1.44	0.005	0.004	-0.01	7.3
Cu-Pd(111)	1.61	14.7	0.97	0.001	0.004	0.02	7.3
Au-Ni(001)	0.87	14.5	1.54	-0.002	-0.019	0.23	14.7
Au-Ni(111)	1.42	16.3	1.17	-0.003	-0.032	0.43	14.7

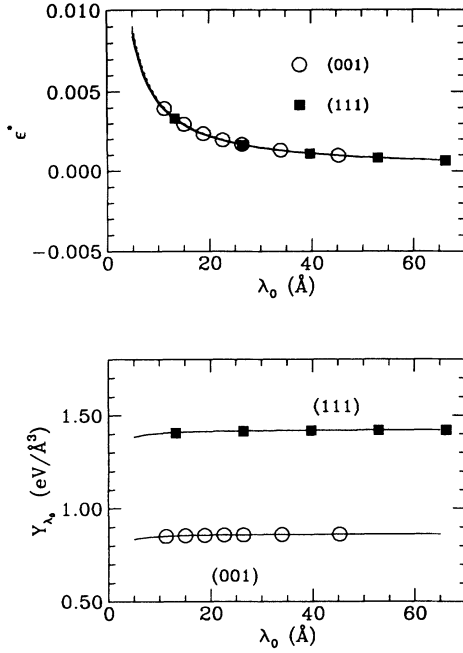


FIG. 6. Equilibrium biaxial strain ϵ^* and biaxial modulus Y_{λ_0} as functions of composition modulation wavelength λ_0 for coherent (001)- and (111)-oriented Au-Ni multilayers.

we presume that the surface modulus acts over a distance on the order of an interlayer separation z_0 , then we can compare the relative importance of f'/z_0 , where z_0 is of order 2 \AA , to Y_∞ , the biaxial modulus. For the Au-Ni system, f' is -0.3 eV/\AA^2 , so f'/z_0 is approximately -0.15 eV/\AA^3 . The biaxial modulus is approximately 1 eV/\AA^3 , so the surface modulus is seen to be on the order of 15% of the biaxial modulus. The region of solid near the interface will, in this interpretation, respond to a stress with an effective modulus which is the sum of the normal modulus and this surface modulus. As the surface moduli which we have measured are negative, this would amount to approximately a 15% softening of the modulus at the surface. There is experimental evidence to support the notion of force-constant softening in noble metals. Estimates range from a 10% to 15% softening in Cu(111), to 47% on (111) Au, all in agreement with the crude picture given above.^{35,36}

B. Noncoherent multilayers

We studied noncoherent Au-Ni and Ag-Ni multilayers using the same Johnson analytic EAM potentials which we had used for the thin films and coherent multilayers. The silver-nickel system was also studied using the universal EAM potentials and the modified form of the analytic EAM potential. The values of Y_∞ , B_∞ , η , f_0 and f' were measured using the techniques described above, and are presented in Table V. The interface stress which develops in the noncoherent Au-Ni system is fairly large (about one-half of a typical free surface stress). Note that the values of f' are much larger than the corresponding values for thin films or coherent multilayers

TABLE V. Values of Y_∞ , B_∞ , η , γ , f_0 , f' determined from simulations of (001) and (111) interfaces of noncoherent Au-Ni and Ag-Ni, as discussed in the text. ($\text{eV/\AA}^3 = 1.6022 \times 10^{11} \text{ J/m}^3$, $\text{eV/\AA}^2 = 16.022 \text{ J/m}^2$).

	Y_∞ (eV/\AA^3)	B_∞	η	γ (eV/\AA^2)	f_0 (eV/\AA^2)	f' (eV/\AA^2)
Au-Ni(001)	1.04	14.6	1.36	0.071	0.037	-0.42
Au-Ni(111)	1.69	15.2	0.98	0.047	0.036	-0.28
Ag-Ni(111) ^a	1.8	15.6	0.64	0.026	0.024	-0.61
Ag-Ni(111) ^b	1.65	15.0	0.77	0.060	0.040	-0.28
"Ag-Ni"(111) ^c	2.07	13.4	0.95	0.093	0.083	-0.90

^aUniversal EAM.

^bAnalytic EAM.

^cModified EAM.

(compare with Tables IV and V). Since f'/f_0 is negative, while B_∞ is positive, we see that the magnitude of f' will reduce the enhancements in Y_∞ due to surface stress in these multilayered systems, as discussed in connection with the coherent Au-Ni samples. Figure 7 displays the equilibrium strain and biaxial modulus as a function of λ_0 for the noncoherent Au-Ni multilayers. The solid lines are plots of the equations for $\epsilon^*(\lambda_0)$ and $Y(\lambda_0)$ given above by Eqs. (1) and (2), respectively. The unexpected nonmonotonic behavior of the shortest wavelength (111) Au-Ni multilayer is consistent with the unexpectedly small value of interface stress measured on this sample. The value of interface stress on the $\lambda_0 = 12.3 \text{ \AA}$ sample is about half that for the other samples. (The other three samples show very little variation in either f_0 or f' among themselves). Were we to use the value of f_0 mea-

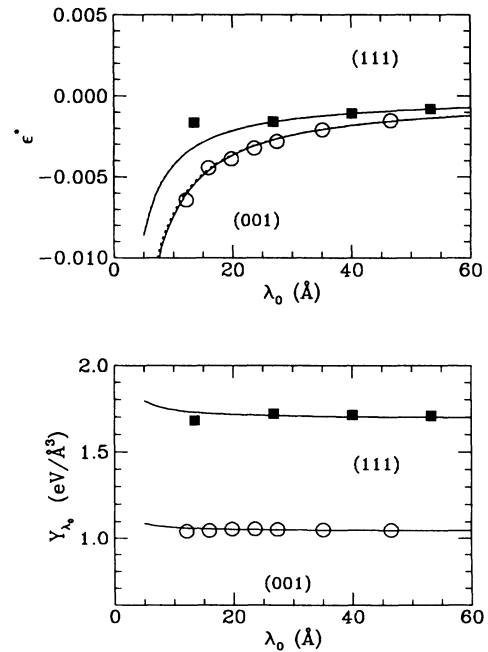


FIG. 7. Equilibrium biaxial strain ϵ^* and biaxial modulus Y_{λ_0} as functions of composition modulation wavelength λ_0 for noncoherent (001)- and (111)-oriented Au-Ni multilayers.

sured on this sample in (2), we would see that the model predicts the variation shown in Fig. 7 quite closely. The interface stress f_0 is expected to be a constant for a particular interface, independent of strain or thickness. We believe that the variation in f_0 which we observed in the (111) Au-Ni samples is a result of the gold and nickel layers each being only three atomic layers thick, so that every atom in the system interacts with the interface. There is no "bulk" region in this sample, a point which we will return to in Sec. VI of this paper.

We studied noncoherent silver-nickel multilayers using the universal EAM potentials, the analytic EAM potentials, and the modified analytic EAM potentials. Figure 8 displays the equilibrium biaxial strain and biaxial modulus as a function of composition modulation wavelength for the Ag-Ni multilayers modeled using each of the potentials. The solid lines are plots of Eqs. (1) and (2) using the values given in Table V. The small strains which develop in the multilayers interacting with the universal EAM potentials are due to the small value of surface stress which they exhibit. The larger value of surface stress attained in the modified potential samples clearly increased the magnitude of the biaxial strain seen in these samples. The "Ag-Ni" multilayers modeled with the modified potential developed strains greater than 0.5% for the thinnest samples, as compared to less than 0.2% strain in the thinnest universal EAM sample. The biaxial moduli of multilayers which were modeled with universal EAM potentials display a reduction of 3.8% with decreasing modulation wavelength. This surprising result comes about because of the larger value of f' in

these films, as in the coherent Au-Ni films mentioned above. Inspection of Table V reveals that the ratio of f' to f_0 is larger in magnitude than B_∞ , and negative. (Note that the small value of f_0 exacerbates this effect.) The simulation results for the analytic potential multilayers show a slight enhancement of 1.6% with decreasing wavelength. In this case the ratio of f' to f_0 is smaller, aided in part by the larger surface stress. The modified potential yielded the largest interface stress and biaxial strains of the three potentials used, suggesting that the modulus would display significant variation with layer thickness. However, by inspecting Table V, we see that the values of the surface modulus f' are also larger for the modified potential samples than in either the analytic potential samples or the universal potential samples. The unexpected increase in f' , coupled with a slight decrease in the value of B_∞ compared to the other potentials, led to a only slight (2.3%) enhancement in the biaxial modulus of (111)-oriented "Ag-Ni" multilayers.

VI. DISCUSSION

The thermodynamic model accurately predicts the biaxial strain and biaxial modulus at equilibrium in thin films and layered structures. We believe that the small differences between the computer simulation results and the prediction of the model through Eqs. (1) and (2) result from surface effects which only become relevant for surfaces which are extremely close together. We did not include these surface effects in the model. The surface stress is the stress which the bulk of the solid must exert on the surface atoms in order to maintain registry. Atoms at a surface will, in general, have different equilibrium in-plane spacings than atoms in the bulk due to their different local environment. As long as the surface does not reconstruct, the surface atoms will maintain coherence with the bulk, so that they share a common in-plane spacing. For surface equilibrium spacings smaller than this shared spacing, the surface atoms are stretched with respect to their own equilibrium spacing, which requires the presence of a tensile surface stress. Likewise, a compressive stress develops if the equilibrium spacing of the surface is larger than the bulk equilibrium spacing. These stresses are parallel to the plane of the surface or interface, and will result in biaxial strains. Strains will develop in the plane of the interface due to forces normal to the interface as well, owing to Poisson effects. As the samples are not constrained in the direction normal to the surface or interface, the layers are free to relax in such a way as to accommodate the normal forces. If the layer becomes sufficiently thin, however, atoms at the two surfaces will start to interact with one another, and it may no longer be possible for the normal forces to be accommodated as they were in a thicker sample. In this case the equilibrium strain state will not be properly described as arising solely due to a biaxial stress. In order to properly analyze extremely thin layers (less than four monolayers thick) we would have to reformulate the model to account for uniaxial stresses normal to the unrelaxed surface. This would entail the addition of a

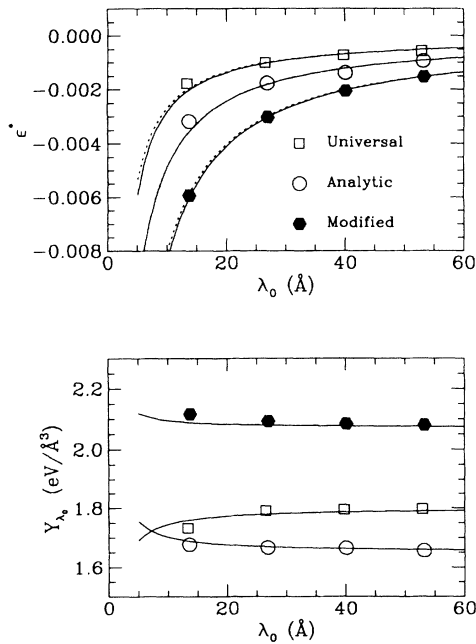


FIG. 8. Equilibrium biaxial strain ϵ^* and biaxial modulus Y_{λ_0} as functions of composition modulation wavelength λ_0 for noncoherent (111)-oriented Ag-Ni multilayers modeled using different forms of the embedded-atom-method potential, as discussed in the text.

ΔU_n term to the energy balance equation [Eq. (1) in I]:

$$\Delta U = \Delta U_{\text{volume}} + \Delta U_{\text{surface}} + \Delta U_{\text{normal}}, \quad (6)$$

where ΔU_{normal} is the work done against a normal force per unit area. By analogy to $\Delta U_{\text{surface}}$, ΔU_{normal} would be given by

$$\Delta U_{\text{normal}} = 2 \int f_n(\epsilon_n) dA(\epsilon_n), \quad (7)$$

where f_n is the normal stress, and ϵ_n is the normal strain. Clearly, such a term would produce a linear contribution to the total-energy equation, Eq. (13) in I. Lacking an f_n term, all biaxial strains will be erroneously attributed to a biaxial stress, since there is no other mechanism for a biaxial strain to appear. Thus, for films so thin that normal stress is not properly accommodated, performing a fit to Eq. (13) in I cannot yield correct values for f_0 .

Let us make an estimate of the change in biaxial modulus predicted by Eq. (2) for real or experimental systems. We estimate the following values as reasonable or typical: $Y_\infty = 1 \text{ eV}/\text{\AA}^3$, $B_\infty = 14$, $\eta = 1$, $f_0 = 0.1 \text{ eV}/\text{\AA}^2$, and $f' = 0.15z_0 Y_\infty$, where $z_0 = 2 \text{\AA}$ is an interplanar spacing. For a wavelength of 20\AA , we would expect a 14% enhancement in the biaxial modulus, due to surface effects. Experimentally, most of the work to date has been done on coherent superlattices, motivated by early reports of a large supermodulus effect. Current reported results for these systems are unanimous in denying the existence of a supermodulus effect.^{7,10,11} Two recent experimental studies reported enhancements in the biaxial modulus for noncoherent metallic multilayer systems, one on an fcc/fcc superlattice⁵ the other on a fcc/bcc multilayer.⁶ Dutcher *et al.* reported enhancement of approximately 14% in the c_{11} elastic constant measured in Ag-Pd multilayers with modulation wavelength below about 60\AA , while Fartash *et al.* reported a 15% increase in the biaxial modulus for Cu-Nb films with wavelength below about 100\AA . Both results agree with the magnitude of effect which we would predict due to interface stress.

VII. CONCLUSIONS

We presented a model which describes the effect that surface and interface stresses have on the structural and elastic properties of metal films and multilayers. The model, originally proposed by Cammarata and Sieradzki, was developed in detail and led to specific predictions concerning the presence of a biaxial strain at equilibrium, and to a biaxial modulus which depends on the film or layer thickness.¹⁸ The equilibrium strain was shown to vary with the magnitude of the surface stress, and inversely with the film or layer thickness. The biaxial modulus was shown to display an inverse thickness dependence which scaled with the magnitude of the surface stress and its derivative with respect to strain, along with higher-order elastic constants. We studied coherent

Cu-Ni, Cu-Pd, and Au-Ni multilayers with either (001) or (111) surface orientations by molecular-dynamics computer simulation using an analytic form of the embedded-atom-method (EAM) potential developed by Johnson.^{25,26} The coherent multilayers were found to have very small values of surface stress, which resulted in virtually no change in biaxial modulus with composition modulation wavelength. The thermodynamic model was again found to yield an extremely accurate description of the changes in modulus and biaxial strain with thickness. Incoherent multilayers of Au-Ni and Ag-Ni were studied by molecular-dynamics simulation using the analytic EAM potentials. The noncoherent interface was shown to have a surface stress substantially larger than seen in the coherent interfaces, amounting to approximately $\frac{1}{2}$ of a typical surface stress on a free surface. The values for f' , or the "surface modulus," were determined to be large and negative at these noncoherent interfaces, resulting in small or negligible variations in biaxial modulus with modulation wavelength. Incoherent Ag-Ni multilayers were also studied using the universal EAM potential of Foiles, Daw, and Baskes²⁴ and a form of the analytic EAM potential which had been modified by the authors to correctly reproduce known values for surface energy and surface stress on Ni and Ag(111) surfaces. The Ag-Ni multilayers were found to display biaxial strains in proportion to the surface stress, as described by the model. The exceptionally large "surface modulus" measured for samples by Foiles, Daw, and Baskes resulted in dehancements in the biaxial modulus with decreasing thickness. Multilayers which were simulated using the modified potential exhibited the largest variation in biaxial modulus, approximately 2.5%. Here again the value of f' was extremely large, effectively canceling the effect of the larger surface stress. Both the analytic and universal EAM potentials were found to yield values of surface energy and surface stress approximately a factor of 2 lower than experimentally observed values or those predicted by *ab initio* calculation for metal surfaces. We presume that interface energies and stresses were similarly reduced from their "true" values. As a result, the enhancements in biaxial modulus observed in our computer study are almost certainly smaller than one might observe in nature, or by using a better set of potentials. Using reasonable estimates for all of the quantities involved, we finally predict that a multilayer formed with noncoherent interfaces whose composition modulation wavelength λ_0 was approximately 20\AA would display an increase in biaxial modulus of about 14% due to interface stress effects. This estimation is in excellent agreement with recent experimental work on the elastic properties of Ag-Pd (Ref. 5) and Cu-Nb (Ref. 6) multilayers. The effect would diminish as $1/\lambda_0$. We conclude by stating that we observed no "supermodulus" effect (modulus enhancements of 100% or more) in either coherent or noncoherent fcc/fcc transition-metal multilayers.³⁷⁻⁴⁰

*Present address: Chemistry Division, Code 6179, Naval Research Laboratory, Washington, D.C. 20375.

¹W. M. C. Yang, T. Tsakalakos and J. E. Hilliard, *J. Appl. Phys.* **48**, 876 (1977).

²T. Tsakalakos and J. E. Hilliard, *J. Appl. Phys.* **54**, 734 (1983); D. Baral, J. B. Ketterson, and J. E. Hilliard, *ibid.* **57**, 1076 (1985).

³G. Henein and J. E. Hilliard, *J. Appl. Phys.* **54**, 728 (1983).

- ⁴H. Itozaki, Ph.D. thesis, Northwestern University, 1982.
- ⁵J. R. Dutcher, S. Lee, J. Kim, G. I. Stegeman, and C. M. Falco, *Phys. Rev. Lett.* **65**, 1231 (1990).
- ⁶A. Fartash, E. E. Fullerton, I. K. Schuller, S. E. Bobbin, J. W. Wagner, R. C. Cammarata, S. Kumar, and M. Grimsditch, *Phys. Rev. B* **44**, 13 760 (1991).
- ⁷A. Moreau, J. B. Ketterson, and J. Mattson, *Appl. Phys. Lett.* **56**, 1959 (1990).
- ⁸J. Mattson, R. Bhadra, J. B. Ketterson, M. Brodsky, and M. Grimsditch, *J. Appl. Phys.* **67**, 2873 (1990).
- ⁹R. C. Cammarata, T. E. Schlesinger, C. Kim, S. B. Qadri, and A. S. Edelstein, *Appl. Phys. Lett.* **56**, 1862 (1990).
- ¹⁰B. M. Davis, D. N. Seidman, A. Moreau, J. B. Ketterson, J. Mattson, and M. Grimsditch, *Phys. Rev. B* **43**, 9304 (1991).
- ¹¹A. Moreau, J. B. Ketterson, and B. Davis, *J. Appl. Phys.* **68**, 1622 (1990).
- ¹²B. W. Dodson, *Phys. Rev. B* **37**, 727 (1988).
- ¹³S. R. Philipot and D. Wolf, *Scr. Metall. Mater.* **24**, 1109 (1990); J. A. Jaszack, S. R. Philipot, and D. Wolf, *J. Appl. Phys.* **68**, 4573 (1990); J. A. Jaszack and D. Wolf, *J. Mater. Res.* **6**, 1207 (1991).
- ¹⁴J. W. Mintmire, *Mater. Sci. Eng. A* **126**, 29 (1990); R. S. Jones, J. A. Slotwinski, and J. W. Mintmire, *Phys. Rev. B* **45**, 13 624 (1992).
- ¹⁵C. M. Gilmore and V. Provenzano, *Phys. Rev. B* **42**, 6899 (1990).
- ¹⁶J. Mei and G. F. Fernando, *Phys. Rev. Lett.* **66**, 1882 (1991).
- ¹⁷G. W. Tecza, *Phys. Rev. B* **46**, 15 447 (1992).
- ¹⁸R. C. Cammarata and K. Sieradzki, *Phys. Rev. Lett.* **62**, 2005 (1989).
- ¹⁹F. H. Streitz, K. Sieradzki, and R. C. Cammarata, preceding paper, *Phys. Rev. B* **49**, 10 699 (1994).
- ²⁰M. Grimsditch, *Phys. Rev. B* **31**, 6818 (1985).
- ²¹M. Grimsditch and F. Nizzoli, *Phys. Rev. B* **33**, 5891 (1986).
- ²²M. Parrinello and A. J. Rahman, *Phys. Rev. Lett.* **45**, 1196 (1980).
- ²³M. S. Daw and M. I. Baskes, *Phys. Rev. B* **29**, 6443 (1984).
- ²⁴S. M. Foiles, M. S. Daw, and M. I. Baskes, *Phys. Rev. B* **33**, 7983 (1986).
- ²⁵R. A. Johnson, *Phys. Rev. B* **37**, 3924 (1988).
- ²⁶R. A. Johnson, *Phys. Rev. B* **39**, 12 554 (1989).
- ²⁷F. H. Streitz, Ph.D. thesis, Johns Hopkins University, 1992.
- ²⁸M. Wüttig, R. Franchy, and H. Ibach, *Z. Phys. B* **65**, 71 (1986).
- ²⁹W. Menezes, P. Knipp, G. Tisdale, and S. J. Siberner, *Phys. Rev. B* **41**, 5648 (1990).
- ³⁰P. Gumbsch and M. S. Daw, *Phys. Rev. B* **44**, 3934 (1991).
- ³¹M. W. Finnis and J. E. Sinclair, *Philos. Mag. A* **50**, 45 (1984).
- ³²R. Rebonato, D. O. Welch, R. D. Hatcher, and J. C. Bilello, *Philos. Mag. A* **55**, 655 (1987).
- ³³J. R. Smith and A. Banarjea, *Phys. Rev. Lett.* **59**, 2451 (1987).
- ³⁴A. Banarjea and J. R. Smith, *Phys. Rev. B* **35**, 5413 (1987).
- ³⁵J. S. Nelson, M. S. Daw, and Erik C. Sowa, *Phys. Rev. B* **40**, 1465 (1989).
- ³⁶V. Bortolani, A. Franchini, F. Nizzoli, and G. Santoro, *Phys. Rev. Lett.* **52**, 429 (1984).
- ³⁷M. S. Daw and M. I. Baskes, *Phys. Rev. Lett.* **50**, 1285 (1983).
- ³⁸G. J. Ackland and M. W. Finnis, *Philos. Mag. A* **54**, 301 (1986).
- ³⁹E. Clementi and C. Roetti, *At. Data Nucl. Data Tables* **14**, 177 (1974).
- ⁴⁰J. H. Rose, J. R. Smith, F. Guinea, and J. Ferrante, *Phys. Rev. B* **29**, 2963 (1984).